Validation of Reduced View-sharing Compressed Sensing Reconstruction for DCE-MRI with Variable Flip Angle Acquisition

Evan Levine[1,2], Bruce Daniel[2], Brian Hargreaves[2], and Manojkumar Saranathan[2]
[1]*Electrical Engineering, Stanford University, Stanford, CA, United States,* [2]*Radiology, Stanford University, Stanford, CA, United States*

INTRODUCTION: Dynamic contrast-enhanced (DCE) MRI entails a tradeoff of spatial and temporal resolution, and schemes using pseudorandom k_y-k_z-t under-sampling trajectories and view-sharing (VS) have been proposed to address this tradeoff.[1-2] Compressed sensing (CS) has shown promise to reduce VS and the temporal footprint of these schemes.[3-5] However, validating these techniques *in vivo* and balancing CS and VS is challenging without a ground truth or the ability to inject contrast twice. In this work, we present a novel approach using a variable flip angle (VFA) acquisition to evaluate sampling and reconstruction strategies. The VFA acquisition is also accelerated with methods used in DCE-MRI. By retrospectively applying the same k-t sampling trajectory and CS/VS schemes used in DCE-MRI to fully sampled VFA data in k-θ space (θ=flip angle), images and signal intensity-flip angle curves were compared to a ground truth dataset *in vivo*. These schemes were also compared using DCE-MRI data from a patient with breast cancer after Gadolinium contrast injection.

METHODS: A fully sampled VFA Dixon bilateral breast acquisition was acquired on a healthy subject with 9 flip angles (θ = 2°–18°) on a GE 3.0T MRI scanner (MR750, GE Healthcare) with a 3D SPGR sequence without contrast injection.[1] Scan parameters: TE1/TE2/TR = 2.2/3.3/6ms, 512×386×192 matrix, 0.8 mm slice thickness. VFA data was retrospectively under-sampled in k-θ space using a pseudorandom trajectory, which samples the central part of k-space (A) and one of four complementary Poisson-disc[7] (CPD) sampling patterns (B_1-B_4) segmented from an outer annular region B for each flip angle (Fig. 1).

Four of the disjoint B regions were view-shared and reconstructed with an autocalibrating parallel imaging method, and one, two, and three nearest-neighbor B regions (i.e. AB_2, B_1AB_2, and $B_4B_1AB_2$) were used in reduced VS reconstructions with joint CS parallel imaging using l_1-ESPIRiT.[8] Accuracy of the four schemes was compared using signal intensity-flip angle curves measured from an ROI (to mimic DCE-MRI signal enhancement) and maps of structural similarity index[9] (SSI) with respect to fully sampled images.

A bilateral breast DCE-MRI acquisition was performed on patients with suspected breast cancer and reconstructed using three schemes (13.0, 20.4, and 46.4 second temporal footprints), and image artifacts and signal intensity-time curves measured from lesion and vessel ROIs were compared in one subject.

RESULTS AND DISCUSSION: l_1-ESPIRiT images from B_1AB_2 data show image quality comparable to that of VS images from VFA (Fig. 1) and DCE (Fig. 2) data. In both cases, ESPIRiT reconstructions without l_1-wavelet regularization showed greater noise amplification (not shown), and l_1-ESPIRiT reconstructions of AB_2 data show blurring artifacts due to high under-sampling in the B region. Images reconstructed from VFA data under-sampled and reconstructed with four VS "temporal" footprints are compared to fully sampled data. SSI maps suggest an optimal balance of CS and VS footprints for signal curves from different T1 species. For example, fast signal changes with θ in fat tissue (light arrow) are require shorter (B_1AB_2) footprints, while slow signal changes near water (dark arrow) require longer footprints (e.g. $B_4B_1AB_2$).

For *in vivo* DCE data, signal intensity-time curves for vessel and lesion ROIs (Fig. 2) show faster contrast uptake with the reduced VS schemes, suggesting better ability to discriminate rapidly enhancing lesions, and the same "temporal" behavior can be seen from signal intensity-flip angle curves. The VFA data can also be replicated, reordered, and/or interpolated to simulate arbitrary contrast uptake curves. For example, responses to a step function are very similar to those from rapidly enhancing lesions (result omitted for clarity).

CONCLUSION: We have proposed a novel method for evaluating data sampling and reconstruction strategies for spatiotemporal imaging applications where a ground truth is not readily available. A full VFA acquisition can simulate arbitrary signal curves and offers a ground truth, which can be used to validate different CS/VS techniques. Results from VFA and DCE data suggest that reduced VS reconstruction with B_1AB_2 data using CS and the CPD trajectory is a suitable alternative to VS reconstruction from $B_3B_4AB_1B_2$ data.

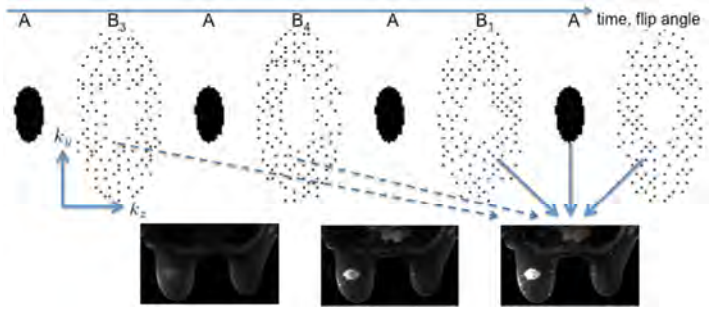

Figure 1: A central region was acquired with each temporal phase or flip angle and complementary Poisson-disc sampling patterns B_1–B_4 segmented from an outer region were interleaved. The footprint of the $B_3B_4B_1AB_2$ VS scheme (solid and dashed arrows) was reduced (e.g. B_1AB_2 data, solid arrows) and data was reconstructed with CS.

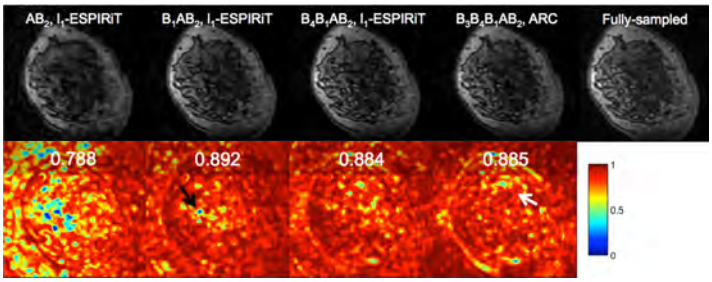

Figure 2: Fully sampled VFA images were compared to images from VFA data retrospectively under-sampled and reconstructed with four VS schemes. SSI maps were used to identify a reduced VS footprint for signal curves from different voxels. Fast signal changes near fat tissue (arrow) require shorter (B_1AB_2) footprints, while slow signal changes near water (arrow) require longer footprints.

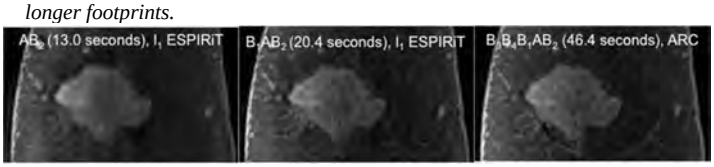

Figure 3: DCE images reconstructed from B_1AB_2 data with CS showed image quality comparable to VS images, enabling a 2.3-fold reduction in temporal footprint. Blurring artifacts were noticeable in AB_2 data with 20x under-sampling in the B region.

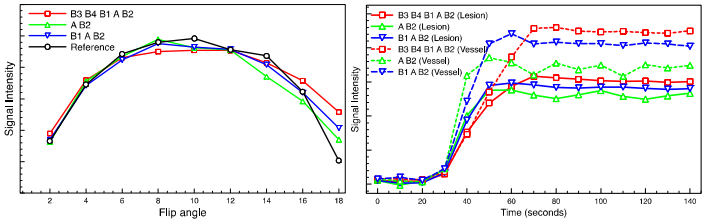

Figure 4: Reduced VS data reconstructed with l_1-ESPIRiT show faster signal changes in VFA data and faster uptake from signal intensity-time courses measured from lesion and vessel ROIs.

REFERENCES: [1] Saranathan *et al*. JMRI 2012; 35:1484-92 [2] Song *et al.* MRM 2009; 61:1242–48; [3] Rapacchi *et al.* MRM 2013 [4] Rapacchi *et al.* ISMRM 2014 [5] Levine E *et al*. ISMRM 2014 [6] Su J *et al.* ISMRM 2012 [6] Levine E *et al.* ISMRM 2014 [7] Uecker *et al.* MRM 2013 [8] Wang, IEEE T-IP 2004

ACKNOWLEDGEMENTS: NIH and GE Healthcare